JOURNAL OF Applied Polymer SCIENCE

Ultrasonic Sealing Versus Heat Conductive Sealing of Polyethylene/Polybutene-1 Peel Films

Michael Nase,[1] Sascha Bach,[2] Armin Zankel,[3] Jens-Peter Majschak,[2] Wolfgang Grellmann[4]

[1]Institute for Polymeric Materials, 06217 Merseburg, Germany

[2]Technical University Dresden, Chair of Processing Machinery and Processing Technology, 01069 Dresden, Germany

[3]Institute for Electron Microscopy, Graz University of Technology, A-8010 Graz, Austria

[4]Martin-Luther-University Halle-Wittenberg, Center of Engineering Sciences, 06099 Halle/Saale, Germany

Correspondence to: M. Nase (E-mail: michael.nase@psm.uni-halle.de)

ABSTRACT: The ultrasonic sealing (USS) is a new and modern possibility to seal peel films for packaging, for example for food and for medical packages. The heat conductive sealing (HCS) in contrast is already well described in science and practice. This study is a comparison of the effectiveness of both the USS and the HCS method using low-density polyethylene/isotactic polybutene-1 peel films. The influence of the recipe of the film, i.e., the amount of the peel component used and the thickness of the peel layer, as well as the sealing parameters, i.e., the sealing temperature, time, and pressure in case of HCS and the sealing force, time, and amplitude in case of USS, on the peel behavior were investigated. To characterize the peel behavior, the peel force, the maximum peel force, and the fracture mechanics, energy release rate were used. The sealing force has a strong impact on the peel properties. This behavior is similar to the influence of the sealing temperature. The peel behavior can be adjusted by varying the content of isotactic polybutene-1. © 2013 Wiley Periodicals, Inc. J. Appl. Polym. Sci. 130: 383–393, 2013

KEYWORDS: adhesives; copolymers; films; structure–property relations

Received 15 October 2012; accepted 17 February 2013; published online 16 March 2013

DOI: 10.1002/app.39171

INTRODUCTION

Films made of blends of low-density polyethylene (LDPE) and isotactic polybutene-1 (iPB-1), with LDPE being the matrix and iPB-1 being the peel component, are the most common peel systems in practice.[1] The functionality of such a peel system is based on the thermodynamic incompatibility between the matrix and the peel component. In other words, the peel component which is the minority phase acts as a kind of microperforation.[2]

Peel systems are often used in packaging, for example for food and drug store packages as well as for packages which include medical equipment to enable easy removal of the packaged goods out of the package. So, peel systems have a broad range of applications because of their convenience in the everyday life, the so-called easy opening. There are a lot of methods to seal (or to weld) such packages. The mostly used welding methods are the heat conductive sealing (HCS), being a thermal welding process, and the ultrasonic sealing (USS), being a frictional or mechanical welding process.[3]

The HCS process and the influence of the sealing parameters on the peel behavior especially of LDPE/iPB-1 peel systems is described in many publications.[4–14] Among the HCS parameters, i.e., the sealing temperature, the sealing time, and the sealing pressure, the processing parameters of the film production[15] and the polymorphism in case of iPB-1[16] strongly affect the peel properties.

Polybutene-1 is a polymorphic polymer, i.e., it exhibit different crystal modifications in dependence on the way of crystallization.[17,18] Crystal polymorphs include forms I, II, and III and forms I′ and II′. Especially, the transformation from form II crystals to form I crystals at ambient temperature is of great practical interest. Melt-crystallization at ambient pressure leads to primary formation of tetragonal form II crystals, which convert at ambient temperature within 6 to 10 days to stable trigonal form I crystals. Along with the II to I crystal transformation, the mechanical properties of iPB-1 changed, e.g., the Young's modulus and the microhardness increase distinctly.[18] Former, own investigations reveal an influence of the II to I crystal transformation on the peel properties of a LDPE/iPB-1 peel system.[16] The peel force decreases exponentially with proceeding II to I transformation of the iPB-1 phase.

It is well known that a defined pressure during sealing is necessary to bring the two films in close contact.[9] The sealing time

Table I. Recipe of the Investigated Peel Films (Total Thickness 80 μm)

Layers	% Composition								
Layer A				20 μm				31 μm	42 μm
LDPE	97.0	94.0	90.0	85.0	80.0	70.0	60.0	94.0	94.0
iPB-1	3.0	6.0	10.0	15.0	20.0	30.0	40.0	6.0	6.0
Layer B				42 μm				31 μm	20 μm
LLDPE	100.0	100.0	100.0	100.0	100.0	100.0	100.0	100.0	100.0
Layer C				18 μm				18 μm	18 μm
Random PP	100.0	100.0	100.0	100.0	100.0	100.0	100.0	100.0	100.0

and the sealing temperature influence the peel properties, for example the peel force, in a similar way. With increasing sealing time or increasing sealing temperature, the peel force also increases.[1,4,9,12] To get a more energetic approach to the peel behavior, fracture mechanics methods and values are used to describe the peel process. For this reason, the adhesive energy release rate was used to emphasize the influence of the recipe of the film on the peel behavior.[19,20]

The USS process is well described in the literature for semicrystalline and also for amorphous bulk materials.[3,21–37] In Ref. 37, the principle and the characteristics of the ultrasonic sealed process of flexible films are described. In opposite to the HCS method in the USS process, the heat is generated inside the material layers or at the interfaces of the thermoplastic materials. The heat generation occurs due to the intermolecular or interfacial friction which in turn is caused by oscillation of the horn and the deformation of the polymer film. Many authors differentiate between USS in the near field, i.e., the distance between horn and sealed interface is less than 6 mm, and USS in the far field, i.e., the distance between horn and sealed interface is more than 6 mm.[22–24] USS in the far field works better for amorphous polymers because the energy dissipation of amorphous polymers in this case is distinctly higher than for semicrystalline polymers. Similar to the HCS process, the USS parameters, i.e., the sealing time, the sealing pressure (or the sealing force in case of a semicircular shape of the energy director), and the sealing amplitude have influence on the seal strength. The seal strength increases with increasing sealing time and/or sealing amplitude. The influence of the sealing pressure is contradictorily discussed in the literature. Benatar et al.[22] stated that the welding pressure (resp. the sealing force) has no influence on the seal strength for their investigated amorphous and semicrystalline materials. In contrast, Shi and Little[38] pointed out that the sealing pressure strongly affects the seal strength. Furthermore, it was found that the seal strength was influenced by the recipe of the film. An addition of organic fillers like calcium carbonate and talc lowers the energy dissipation and consequently decreases the seal strength of the sealed parts.[31] Another point which also influences the energy dissipation and therefore the seal strength in case of USS is the shape of the energy director. Chuah et al.[24] found that a semicircular shape of the energy director leads to highest seal strength compared with the use of a rectangular or triangular shape.

However, up to now, USS of peel films to get a good peel system is not part of any scientific literature. Therefore, in this study, it is intended to investigate the peel behavior of USS LDPE/iPB-1 peel systems in comparison with heat conductive peel systems. Furthermore, the influence of the sealing pressure (or sealing force) on the peel behavior is investigated to clarify the contradictory results within the literature.

EXPERIMENTAL

Materials

Coextruded films of three layers were investigated in this study. The films consist of a peel layer, a standard core layer containing linear low-density polyethylene (LLDPE) and a standard back layer containing random polypropylene (PP) to simulate a laminated film (seal film laminated against a stiff film). The content of iPB-1 of the peel layer was varied between 3 and 40 wt % and the thickness of the peel layer was varied between 20 and 42 μm (Table I).

The blend components of the peel layer LDPE and iPB-1 were commercial polymers, provided by LyondellBasell (Germany). The LDPE used was Lupolen 2420F, which was designed for film production including blowing process. The density is 0.923 g cm^{-3}, and the melt-flow index, determined at 190°C with a load of 2.16 kg, is 0.73 g $(10\ min)^{-1}$. The iPB-1 of this study was PB 8640M. It was a statistical copolymer with a low amount of ethylene, and for primary use as minority blend component for blown film extrusion. The melt-flow index, also determined at 190°C with a load of 2.16 kg, is 1.0 g $(10\ min)^{-1}$. The LLDPE used was LLDPE 118 NE and is a commercial polymer provided by Sabic (Saudi Arabia). The density is 0.918 g cm^{-3}, and the melt-flow index, determined at 190°C with a load of 2.16 kg, is 1.0 g $(10\ min)^{-1}$. The PP used was Borclear RB 709 CF-01 and is provided by Borealis (Austria). The density is 0.905 g cm^{-3}, and the melt-flow index, determined at 230°C with a load of 2.16 kg, is 1.5 g $(10\ min)^{-1}$.

The films were processed at Orbita-Film GmbH using laboratory equipment (Collin, Germany) and a set of standard processing parameters (Table II).

Instrumentation

Light Microscopy. To investigate the flow of the melt in the end of the sealing process, a postmortem analysis using light microscopy was done. A DMRX microscope from Leica (Germany) was used for collection of images in transmission mode.

Transmission Electron Microscopy. The structure of the peel films was analyzed by transmission electron microscopy (TEM).

Table II. Conditions of Processing Blown Films of Blends of PE-LD and iPB-1

Extruder parameters	Maddock mix and shear elements
	100 rpm screw speed
	Temperature profile: 140°C–160°C–180°C–180°C–180°C
Die head parameters	Temperature profile: 180°C–180°C–180°C–180°C
	Die gap: 0.8 mm
Tube formation	Time of solidification 1.8 s
	Blow-up ratio 1:2
	Draw-down ratio 1:7.85

Therefore, a LEO 912 microscope (ZEISS, Germany) was used, which operated at 120 kV. The bulk material was stained with RuO_4. Afterward, thin sections of thickness of about 80 nm were prepared using an Ultracut E (Reichard, Germany) microtome. The samples were oriented such that the images show the structure of the MD-ND cross-section, with MD being the machine direction, i.e., the direction of extrusion, and ND being the direction of the normal of the surface of the blown-film.

HCS. The peel films were sealed together achieving a peel system using standard sealing parameters, i.e., the sealing time was 0.2 s, the sealing pressure was 1 MPa, and the sealing temperature was 140°C. During the investigations, the sealing temperature was varied between 110 and 150°C. After sealing, the films were stored 10 days in the laboratory to enable full transformation from crystal form II to I of the iPB-1.

USS. The peel films were sealed together using an USS process with standard parameters. The sealing time was 0.2 s, the sealing amplitude was 30 μm, and the sealing force was 1000 N (width of the seal bar was 200 mm). The parameters selected are close to most packaging processes. Because of the use of a semicircular energy director, it is not easy to calculate a sealing pressure from the line-force used. Therefore, we decided to use the sealing force, even if it is not fully comparable with other systems. The sealing force was varied between 400 and 1200 N. We did the USS tests in the near field, i.e., the distance between horn and joint/sealed interface was less than 6 mm.[22] After sealing, the films were stored 10 days in the laboratory to enable full transformation from crystal form II to I of the iPB-1.

T-Peel Test. The T-peel test according to ASTM D 1876[39] was applied to investigate the peel behavior of the peel films produced with variable processing conditions. A schematic of the T-peel test including sample geometry, and direction of loading respective to sample orientation, is shown in Figure 1. A Zwicki tensile-testing machine (Zwick, Germany) was used for this test. The initial distance between the clamps was 50 mm, and the standard peel rate was 100 mm min^{-1}. The recorded data, force as a function of elongation, were used to determine the peel force F_{peel}, which is defined as average force between 20% and 80% of the elongation at break (the plateau-like part of the curve progression only in case of HCS)[19] and the maximum peel force (in case of USS and HCS), which is defined as maximum force within the recorded force-elongation data (Figure 2). In case of USS, it was not possible to calculate the (average) peel force, because of the missing of a plateau-like part of the force–elongation data.

Furthermore, the fracture mechanics parameters of the peel process were calculated as follows. The energy release rate G_{Ic} according to Irwin[40] is given by eq. (1), where E_G is the total peel energy, which corresponds to the area under the force–elongation diagram (peel curve) up to the break, W is the width of the seal area, and L is the length of the seal area.

$$G_{Ic} = \frac{E_G}{WL} \tag{1}$$

Among the energy release rate, the adhesive fracture energy release rate G_{aIc} (adhesive energy release rate) was determined following eq. (2) to consider the deformation energy of the peel arm $E_{d,P}$ and the deformation energy of the peeled seal area $E_{d,S}$ to achieve only that energy which is necessary to separate the seal area of the two sealed films.

$$G_{aIc} = \frac{E_G - E_{d,P} - E_{d,S}}{WL} \tag{2}$$

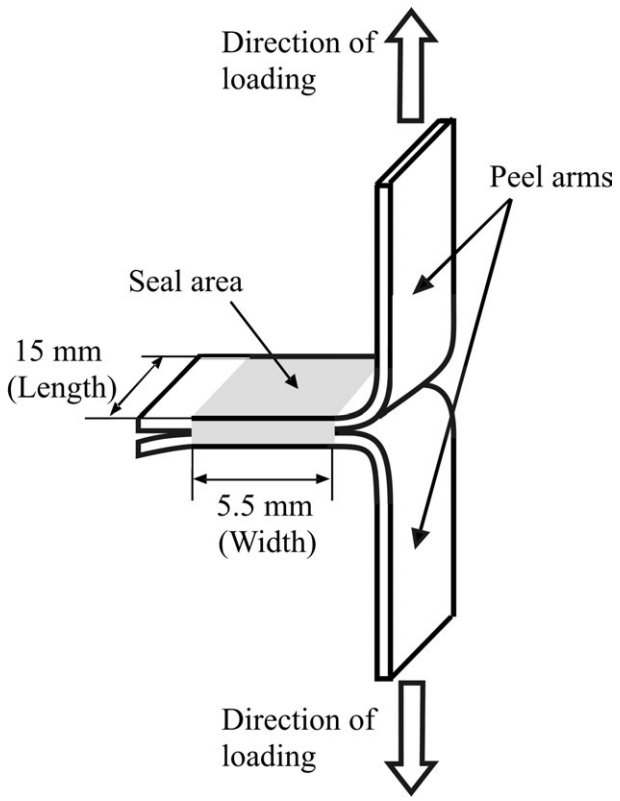

Figure 1. Schematic of the T-peel test. The gray area represents the seal area, which was sealed at 140°C, for a period of time of 2 s and, subsequently, cooled in air.

Applied Polymer SCIENCE

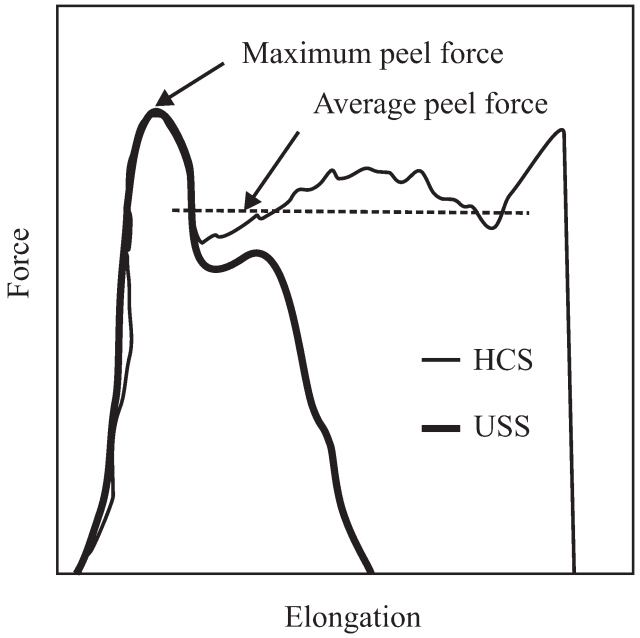

Figure 2. Schematic of the recorded data, force as a function of elongation, that is used to determine the peel force, which is defined as average force between 20% and 80% of the elongation at break (the plateau-like part of the curve progression only in case of HCS) and the maximum peel force (in case of USS and HCS), which is defined as maximum force within the recorded force–elongation data (HCS—heat conductive sealing, USS—ultrasonic sealing).

A description of the calculation of the energy release rate and the adhesive fracture energy release rate is shown elsewhere.[19]

***In Situ* T-Peel Test.** The *in situ* T-peel test was applied for simultaneous structural and mechanical investigations of the proceeding peel process at ambient temperature. The performance of the *in situ* T-peel test is similar to the performance of the T-peel test outside the environmental scanning electron microscopy (ESEM).[19,39] A microdeformation device (MT5000 from Deben; Suffolk, UK), which was mounted in the sample chamber, was used for this *in situ* peel test. The microdeformation device and, even more, the peel film samples were placed in the sample chamber in such a manner, that an observation of the peeling seal area is possible (Figure 3). Therefore, the microdeformation device draws the peel film symmetrically. The initial distance between the clamps was 42.5 mm, and the peel rate was 1 mm min^{-1}. The simultaneous record of the ESEM images and the mechanical data (force–elongation data, peel curve) enables the direct establishment of structure–property relationships. The peel force F_{peel}, the energy release rate G_{Ic} and the adhesive fracture energy release rate G_{aIc} were calculated in the same way as using the T-peel test outside the ESEM chamber.

The *in situ* investigations were performed in an ESEM Quanta 600 FEG from FEI (Eindhoven, The Netherlands), working in the low vacuum mode (nominally about 13.3–333.3 Pa). The specific imaging principle of the ESEM, which enables the investigation of nonconducting specimens, is described elsewhere.[41] In this study, the high voltage was 10.0 kV, the pressure of the imaging gas (water vapor) was 66.7 Pa, and the working distance was about 11.3 mm, respectively.

RESULTS AND DISCUSSION

Structure of the LDPE/iPB-1 Peel Films

The structure of the investigated LDPE/iPB-1 peel films is shown in Figure 4. Two polymer phases could be observed, the elongated particles being the iPB-1 phase and the surrounding matrix being the LDPE phase. Within the LDPE phase, the brighter regions are the amorphous phase and the darker regions are the crystalline phase. Furthermore, the TEM images reveal crystallization of LDPE in terms of lamellae. The internal structure of iPB-1 could not be clearly seen. The iPB-1 particles are elongated in machine direction, the direction of extrusion. The LDPE lamellae are preferably oriented with their long axis perpendicular to the machine direction. Thus, the c-axis, which can be considered as the direction parallel to the polymer chain is oriented parallel to the machine direction.

Among the general polymeric phase structure, an ingrowth of the LDPE lamellae into the iPB-1 particles could be observed. Even the two polymers are thermodynamically incompatible, they exhibit a small shared boarder. This ingrowth could be due to the low amounts of ethylene within the iPB-1. The used iPB-1 (PB 8640M) is a butene-1-ethylene-copolymer.

Influence of the Sealing Parameters

The relation between sealing time, sealing temperature, sealing pressure, and peel behavior in case of HCS is well established. For USS films, we could also prove a distinct influence of the sealing amplitude and the sealing time on the peel properties as it is shown in the literature.[22] Furthermore, the influence of the sealing force on the peel behavior in case of USS peel films was analyzed and directly compared with the sealing temperature

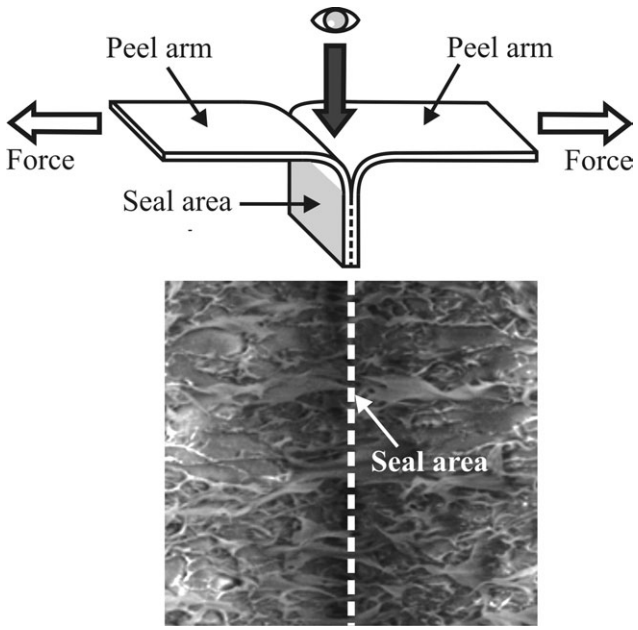

Figure 3. Schematic of the observation process of the peel film samples within the ESEM sample chamber. It is a direct view into the peeling seal area.

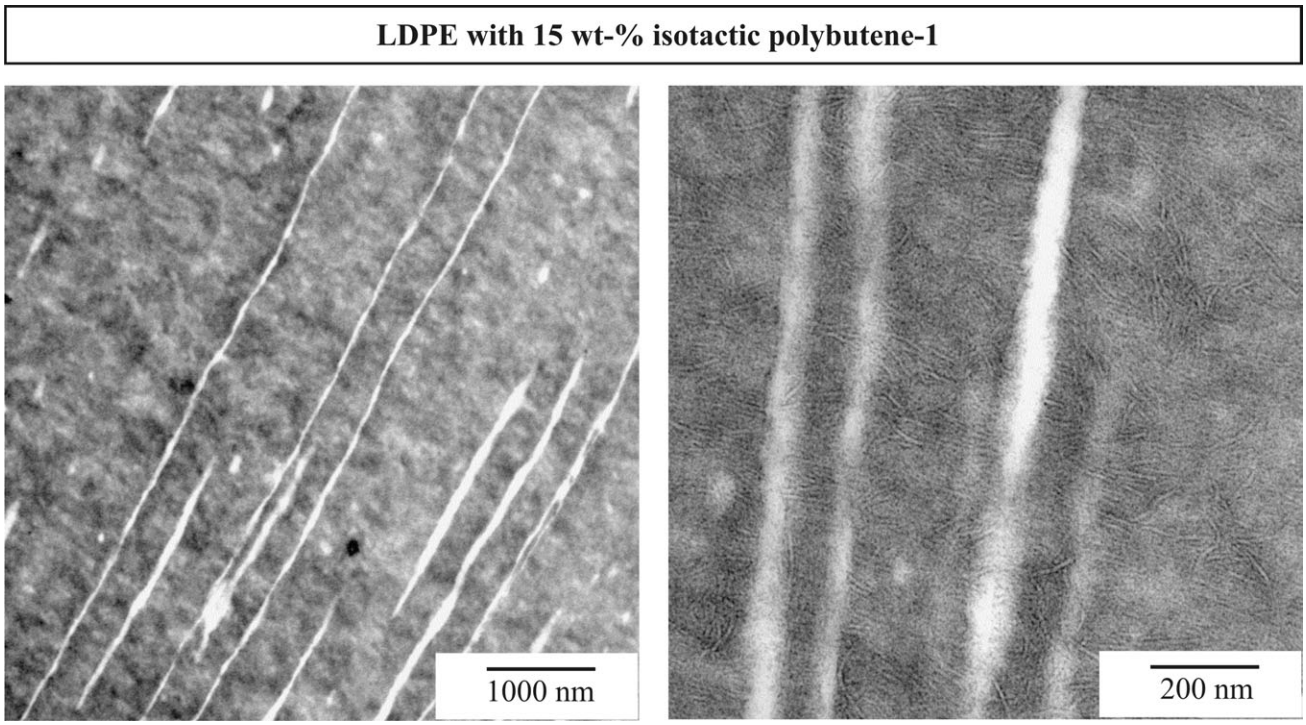

Figure 4. TEM images of LDPE with 15 wt % iPB-1, overview (left image), detailed view (right image).

which has an amazing impact on the peel properties in case of HCS peel films while keeping the sealing time and others constant. Before such a comparison was possible using energy determined fracture mechanics values, the percentage of energy, which is directly used for the peel process, in comparison with the energy, which is used to elongate the peel arms and/or the peeled seal area, has to be ruled out. Therefore, the relation between adhesive energy release rate (which considers only the peel energy) and energy release rate (which considers the total energy used, including elongation of the peel arms and elongation of the peeled seal area) was plotted in dependence on content of iPB-1 using HCS peel films (Figure 5). The data reveal that starting at 15 wt % iPB-1 the influence of the deformation of the peel arms and of the deformation of the peeled seal area is $\sim$ zero. This is very important because it was not possible to calculate the adhesive energy release rate for USS peel films. The force–elongation data of USS peel films did not give any indication for the deformation of the peel arms or the peeled seal area. However, if peel films were used with a content of iPB-1 greater than 15 wt %, only a negligible influence of the parts of deformation energy of the peel arms and peeled seal area has to be considered. Figure 6 shows the direct comparison of the influence of the sealing temperature (HCS) and the sealing force (USS) on the energy release rate for 15 wt % (a) and 30 wt % iPB-1 (b). The data point out that the selected ranges of the sealing force and the sealing temperature are directly comparable because they seem to have the same impact on the energy release rate. This result is in accord with Shi and Little,[38] who also found a distinct dependence of the sealing force on the bond strength (or sealing strength). After evidencing the direct comparability of the sealing temperature in case of HCS and of the sealing force in case of USS in the ranges selected, the influence of both sealing parameters on the maximum peel force, i.e., the most common value in engineering practice to describe the peel behavior was investigated. Figure 7(a) shows the maximum peel force as a function of the sealing temperature for LDPE with 6, 15, and 30 wt % iPB-1. With increasing sealing temperature, the maximum peel force also increases. The higher the sealing temperature, the lower the relative impact on the maximum peel force. This asymptotic behavior is caused by

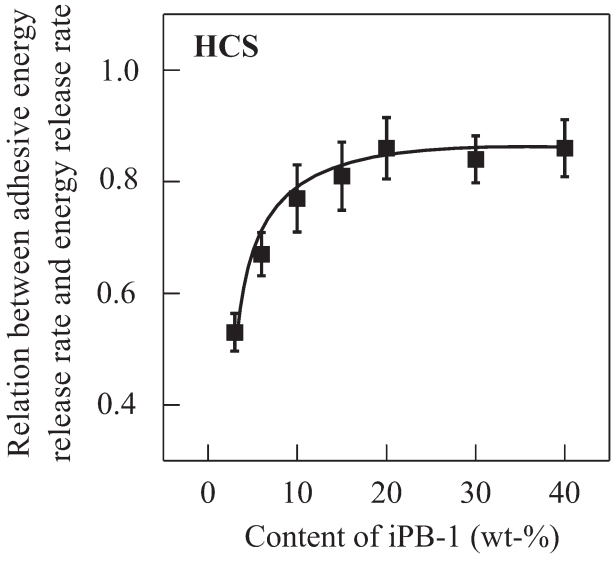

Figure 5. Relation between adhesive energy release rate and energy release rate in dependence on content of iPB-1 using HCS peel films.

Applied Polymer SCIENCE

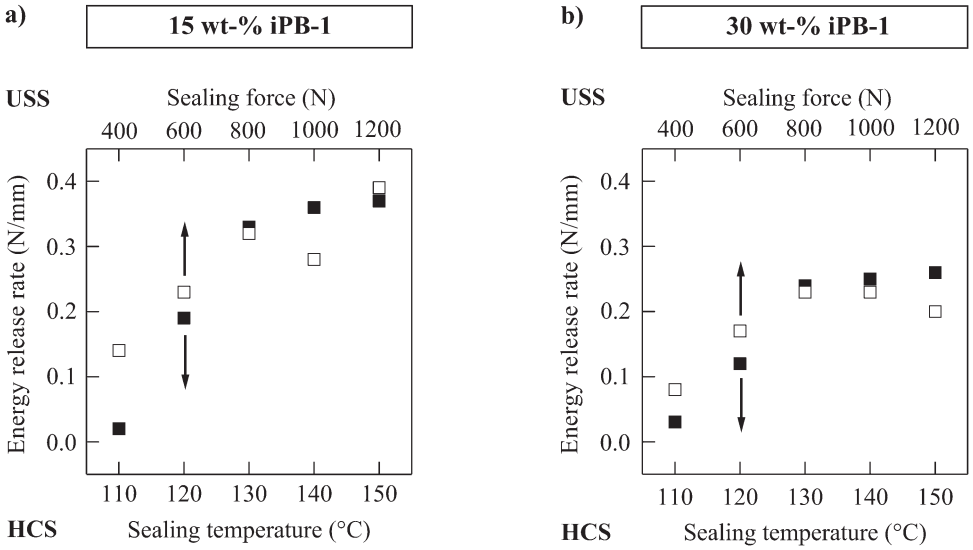

Figure 6. Energy release rate as a function of the sealing temperature using HCS films and as a function of the sealing force using USS peel films with a content of iPB-1 of 15 wt % (a) and 30 wt % (b).

the interpenetration of molecular chains at the interface of the two sealed films which is not endless increasable.[36] Thus, the high temperatures selected lead to an interpenetration status near the possible maximum. The plotted data also reveal a more distinct dependence of the maximum peel force on the sealing temperature for lower contents of iPB-1. In comparison with that, the sealing force in case of USS, influences the maximum peel force in a similar way to the sealing temperature in case of HCS [Figure 7(b)]. One main difference between both sealing processes can be observed for high values of sealing temperature and sealing force, respectively. For high sealing forces, the maximum peel force shows a further slope in contrast to high sealing temperatures. This phenomenon is based on the different sealing techniques. The HCS applies heat on the film and the heat, which is related to the total energy input, leads to an interpenetration of the molecular chains at the interface of the two adhered films. However, the USS applies a repeating mechanical load on one side of the two films. This leads to a melting of the two polymeric films at their interface as a consequence of the inner friction due to the frequently mechanical load. However, this mechanical load also leads to a melt-flow to the border of the seal area. So, the seal area becomes thinner in its middle. If the sealing force is high enough, the seal layer is completely outside the seal area, which causes a nonpeelable seal of the two midlayers of the peel films adhered. This is the reason for the further slope of the maximum peel force for relatively high sealing forces as it is shown in Figure 7(b). To evidence this effect aforementioned, the width of the seal area using different sealing forces was measured which is shown in Figure 8(a–e). The width of the seal area increases with increasing sealing force by a linear law [Figure 8(f)]. This has to be considered calculating the fracture mechanics values. Among the increase of the width, a change of the alignment of the border of the seal area can be observed. For high sealing forces, the border of the sealing area gets more and more waved. This is also an indication of the melt-flow outside the center of the seal

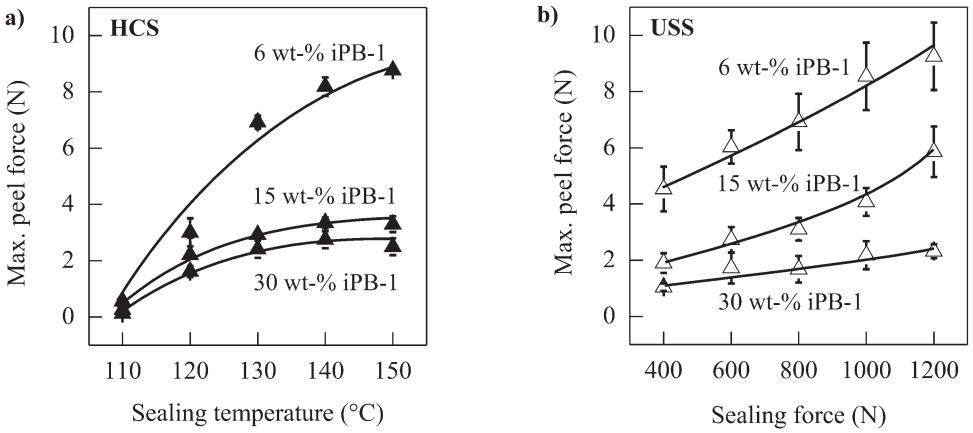

Figure 7. Maximum peel force in dependence on the sealing temperature using HCS (a) and USS (b) peel films with various content of iPB-1 of 6, 15, and 30 wt %.

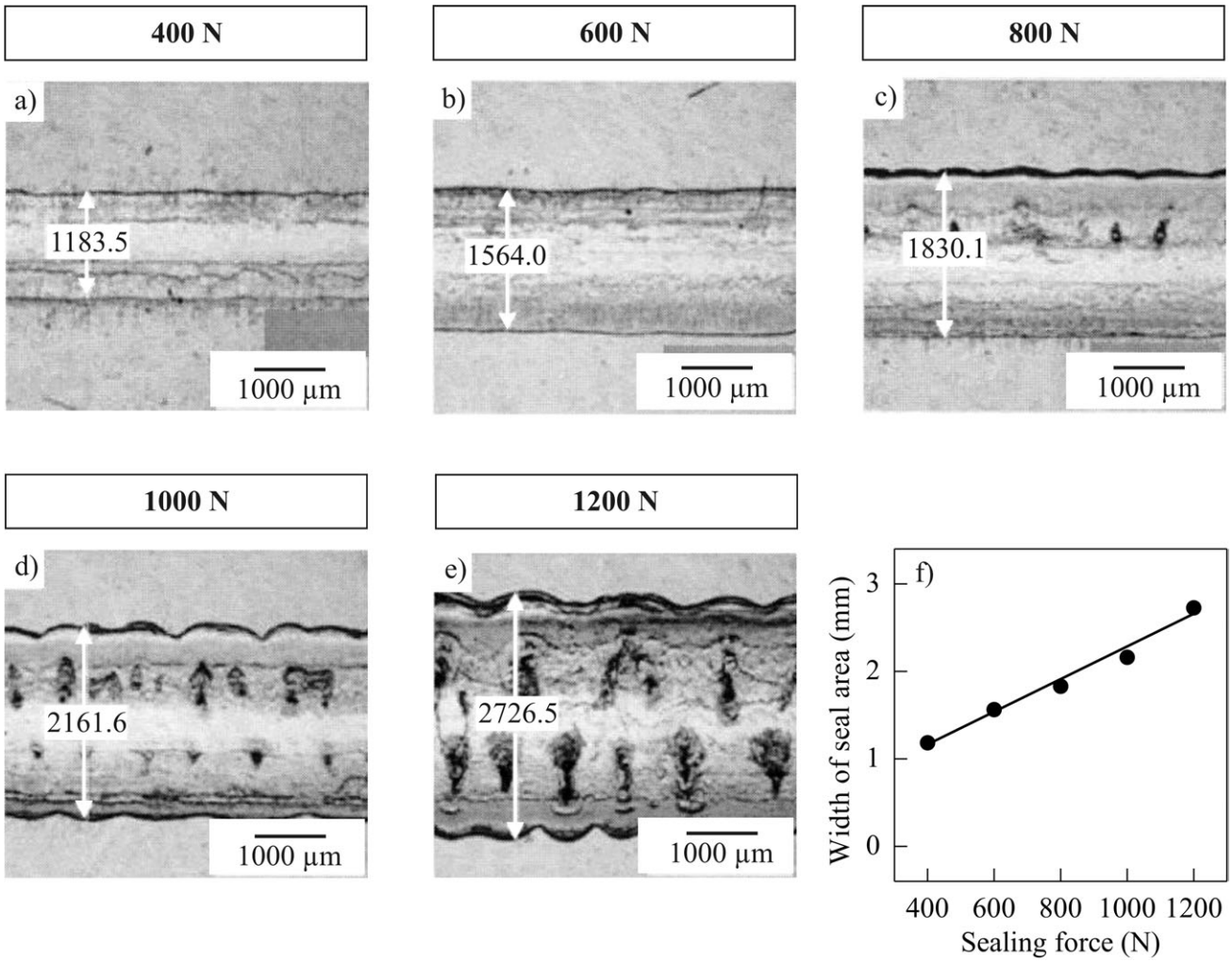

Figure 8. Light microscopy images of the cross-section of the middle of the seal area of PE-LD/iPB-1 peel films with 6 wt % iPB-1, which were sealed using USS process, varying the sealing force (a–e) and the resulting width of the seal area in dependence on the sealing force (f).

area. A further evidence for this effect is given by the microscopic image of the cross-section of the seal area (Figure 9). Between the two peel arms, a melt agglomeration was found. This melt originally comes out of the seal area due to the mechanical loading of the USS process.

Influence of the Recipe of the Peel Film

The influence of the recipe of the film, i.e., the content of iPB-1 and the thickness of the peel layer, on the peel behavior was investigated. Figure 10 shows the peel force, the maximum peel force, and the energy release rate in case of HCS peel films (a), and the maximum peel force and the energy release rate in case of USS peel films (b) in dependence on the content of iPB-1. The measured values as well as the fracture mechanics values decrease exponentially with increasing content of iPB-1 for both sealing processes used. Therefore, the content of iPB-1 could be varied to adjust a specific peel behavior of the peel film for HCS and USS peel films. This knowledge in general is very important for industrial practice because the HCS peel films can be possibly replaced with USS ones. However, the standard deviation for the fracture mechanics values in case of USS peel films and even more for the measured value of maximum peel force is relatively high in comparison with the values for HCS peel films. This effect is highly intensive for amounts of iPB-1 of less than 10 wt %. During the USS, the molten sealing layer went out of the center of the sealing area (in extreme case) (cf., Figure 9). Because of this mobility of the molten sealing layer, the dispersion of the iPB-1 particles is not homogeneous after re-cooling of the sealing area. In contrast, the HCS is very smooth. The process takes place without any dynamic loading. The sealing occurs only due to the sealing temperature and/or time. That is the reason why the iPB-1 particles are dispersed homogeneously, using HCS. Variations of the dispersion and/or dosing of the iPB-1 phase of LDPE with low amounts of iPB-1, generally lead to high impact on the peel properties, e.g., the peel force as revealed by Figure 10. Thus, high amounts of iPB-1 within the LDPE/iPB-1 peel film can compensate the change of the dispersion of iPB-1, as a consequence of the dynamic USS. The ESEM images, which are shown in Figure 11, are a good indication for that pronouncement. The images of USS peel films (bottom row) show distinct inhomogeneous plastic deformations, which can be definitely the result of an

Applied Polymer SCIENCE

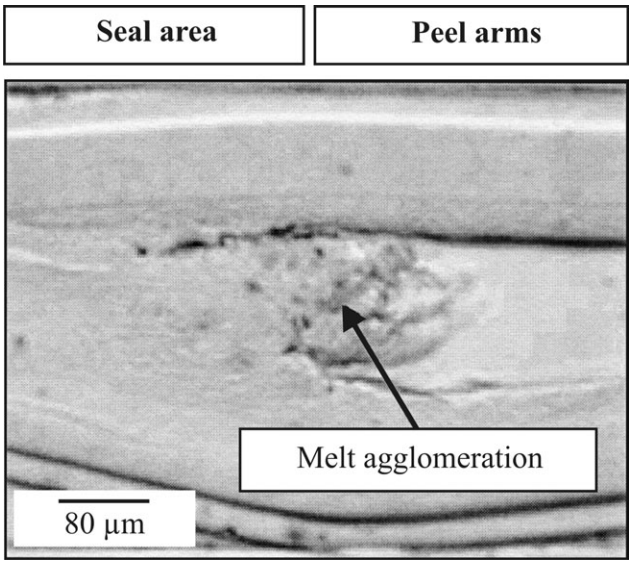

Figure 9. Light microscopy image of the cross-section of the boarder of the seal area of PE-LD/iPB-1 peel film with 6 wt % iPB-1, which were sealed using USS process.

inhomogeneous dispersion of iPB-1 particles. In contrast to that the plastic deformations of HCS peel films (top row) are of a homogeneous alignment, which could be expected from earlier results.[2] The ESEM images also reveal a change or a difference of the level of inhomogeneity from 6 wt % to 20 wt % iPB-1 in case of USS peel films (bottom row). The inhomogeneous plastic deformations are marked by white arrows. The higher level of inhomogeneity for 6 wt % iPB-1 leads to the high standard deviation (cf., Figure 10) in contrast to the lower level of inhomogeneity for 20 wt % iPB-1 in case of USS peel films. Among the variation of the content of iPB-1, the thickness of the peel layer is of great practical interest. From economic point of view, the peel layer has to be as small as possible because of the use of expensive peel components. For that reason, the influence of the peel layer thickness on the peel behavior of LDPE with 6 wt % iPB-1 was investigated. Figure 12(a) shows an increase of the maximum peel force and the energy release rate with increasing thickness of the peel layer for HCS peel films. This increase is based on the different alignment of the iPB-1 particles for different peel layer thicknesses as a consequence of different shear behavior. The high shear rate in the thinnest peel layer causes small iPB-1 particles with a high aspect ratio, whereas the lower shear rate in the thickest peel layer causes large iPB-1 particles which in turn leads to a higher peel force and higher energy input. The dependence of the energy input, i.e., the energy release rate, on the peel layer thickness is of exponential character. Therefore, peel layer thicknesses higher than 42 μm cause no higher energy input and consequently no higher (maximum) peel force. The dependence of the maximum peel force and the energy release rate for USS peel films is shown in Figure 12(b). The data reveal no clear tendency because of the high standard deviation. However, the maximum peel force and the energy release rate seem to be independent from the peel layer thickness. An observation of the microstructure of the LDPE/iPB-1 peel film during the peel process (Figure 13) gives the reason for the high standard deviation. Similar to Figure 11 (bottom row), the inhomogeneous plastic deformation (cf., Figure 13, bottom row) as a consequence of the inhomogeneous dispersion of iPB-1 particles as well as a result of the dynamic USS process causes that high standard deviation and the less reproducibility of the peel behavior for a peel layer thickness of 20 μm (left column) as well as 42 μm (right column).

CONCLUSIONS

The experimental investigation of the influence of sealing conditions on the peel behavior, in particular the peel force, the maximum peel force, and the fracture mechanics energy release rate, of sealed LDPE/iPB-1 peel films was reported in this study. Among the sealing conditions, the variation of the recipe of the peel film, i.e., the content of iPB-1 and the thickness of the peel layer, was investigated.

As a result of the investigations, it can be stated that the sealing force, in case of USS peel films, and the sealing temperature, in case of HCS peel films, have a strong impact on the peel properties. During USS, a melt-flow outside the center of the seal area takes place (especially for high sealing forces). That causes less reproducibility because in extreme cases the sealing process involves the two midlayers, which lead to a nonpeelable seal. The possibility to adjust the peel behavior by varying the

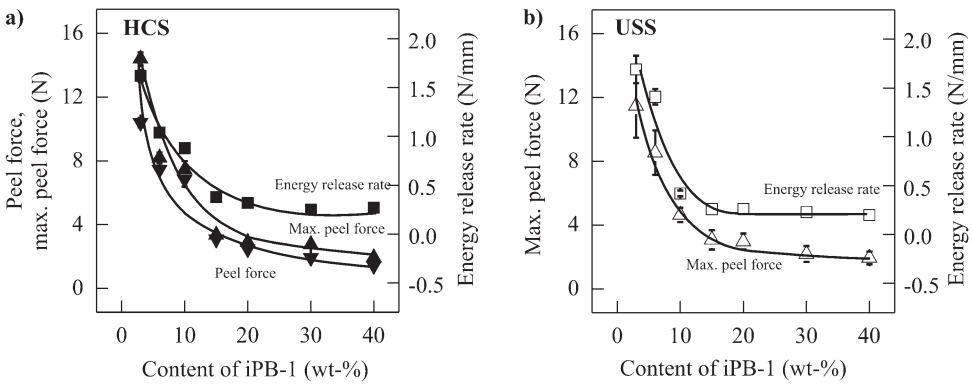

Figure 10. Peel force, maximum peel force, and energy release rate as a function of iPB-1 content for HCS peel films (a) and maximum peel force and energy release rate as a function of iPB-1 content for USS peel films (b).

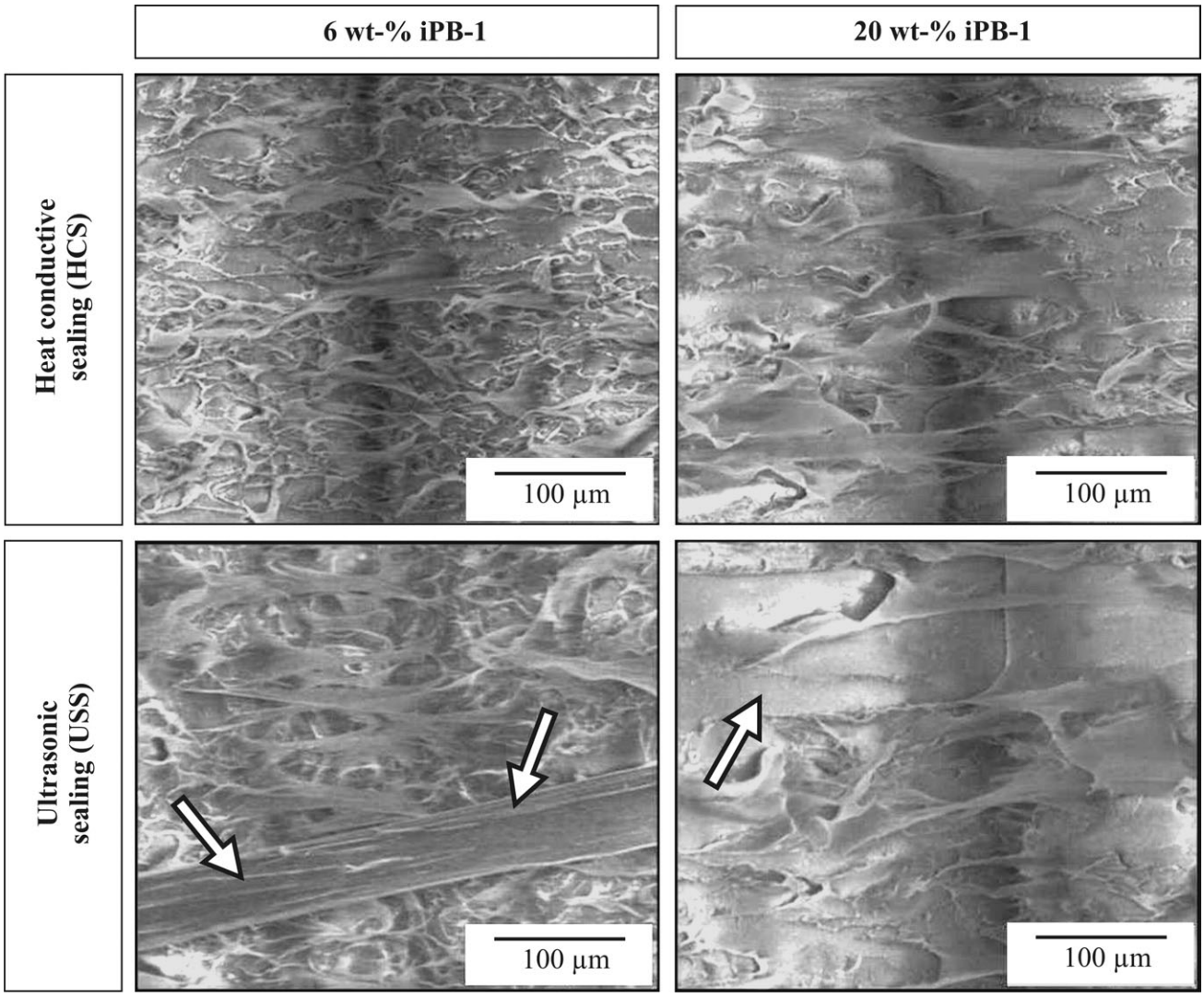

Figure 11. Scanning electron microscopy images (low vacuum mode of the ESEM) of PE-LD/iPB-1 peel films with 6 wt % iPB-1 using HCS (top, left) in comparison with USS (bottom, left) and ESEM images of PE-LD/iPB-1 peel films with 20 wt % iPB-1 using HCS (top, right) in comparison with USS (bottom, right).

content of iPB-1 is independent from the sealing method, HCS or USS. Furthermore, the variation of the thickness of the peel layer is of economic interest, because the peel component used is the most expensive component of the peel film. The higher the thickness of the peel layer, the higher the maximum peel force and the energy release rate. Therefore, a cost-efficient

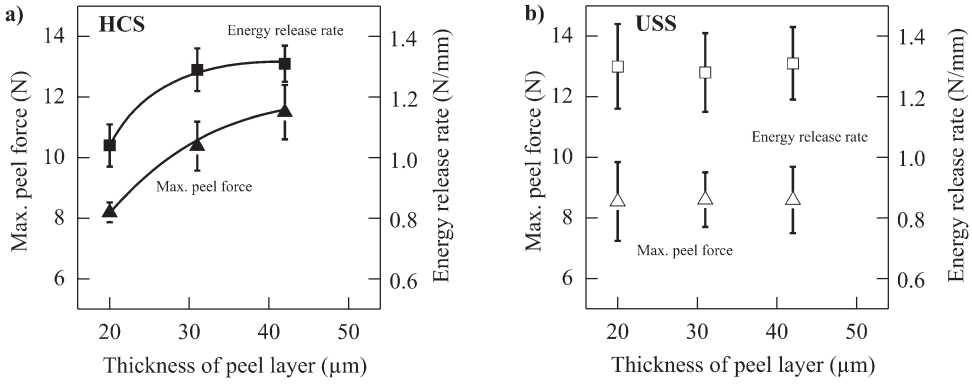

Figure 12. Maximum peel force and energy release rate as a function of the thickness of the peel layer for HCS peel films (a) and for USS peel films (b) of LDPE with 6 wt % iPB-1.

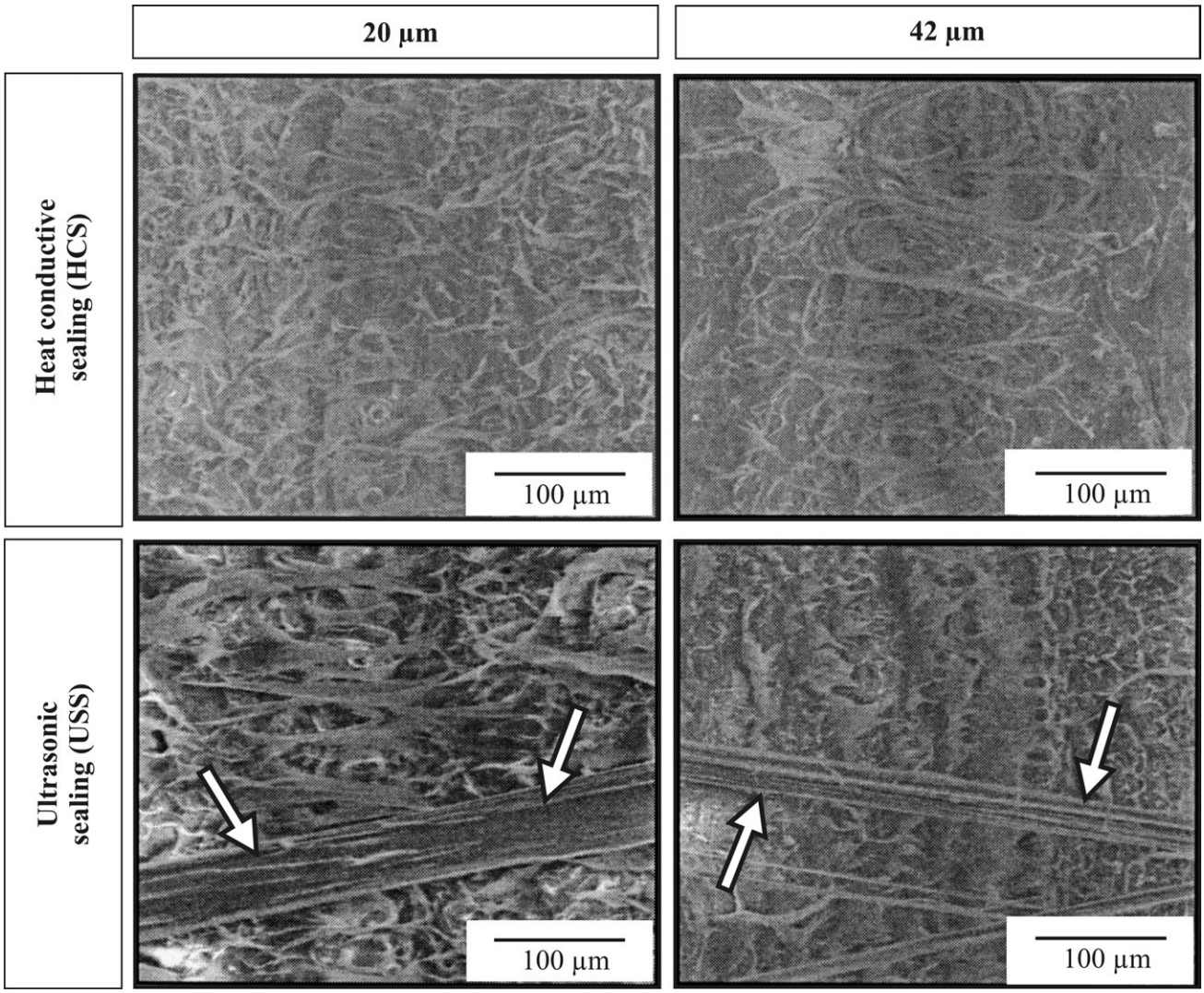

Figure 13. Scanning electron microscopy images (low vacuum mode of the ESEM) of PE-LD/iPB-1 peel films with a peel layer thickness of 20 μm using HCS (top, left) in comparison with USS (bottom, left) and ESEM images of PE-LD/iPB-1 peel films with a peel layer thickness of 42 μm using HCS (top, right) in comparison with USS (bottom, right).

construction of the peel film with a low thickness of the peel layer leads to low peel level. In other words, using thin peel layers, a reduction of the content of iPB-1 is possible to get similar peel properties than using a large peel layer thickness and a high amount of iPB-1. In case of USS peel films, the peel properties seem to be independent of the peel layer thickness.

REFERENCES

1. Hwo, C. C. *J. Plast. Film Sheeting* **1987**, *3*, 245.
2. Nase, M.; Zankel, A.; Langer, B.; Baumann, H. J.; Grellmann, W.; Poelt, P. *Polymer* **2008**, *49*, 5458.
3. Stokes, V. K. *Polym. Eng. Sci.* **1989**, *29*, 1310.
4. Aithani, D.; Lockhart, H.; Auras, R.; Tanprasert, K. *J. Plast. Film Sheeting* **2006**, *22*, 247.
5. Bonten, C.; Schmachtenberg, E. *Polym. Eng. Sci.* **2001**, *41*, 475.
6. Geißler, G.; Kaliske, M.; Nase, M.; Grellmann, W. *Eng. Comp.* **2007**, *24*, 586.
7. Kinloch, A. J.; Lau, C. C.; Williams, J. G. *Int. J. Fract.* **1994**, *66*, 45.
8. Kinloch, A. J.; Williams, J. G. In Adhesion Science and Engineering; Dillard, D. A.; Pocius, A. V., Eds.; Elsevier, **2002**; Chapter 8, pp 273–301.
9. Meka, P.; Stehling, F. C. *J. Appl. Polym. Sci.* **1994**, *51*, 89.
10. Nase, M.; Langer, B.; Baumann, H. J.; Grellmann, W.; Geißler, G.; Kaliske, M. *J. Appl. Polym. Sci.* **2009**, *111*, 363.
11. Nase, M.; Funari, S. S.; Michler, G.; Langer, B.; Grellmann, W.; Androsch, R. *Polym. Eng. Sci.* **2010**, *50*, 249.
12. Stehling, F. C.; Meka, P. *J. Appl. Polym. Sci.* **1994**, *51*, 105.
13. Yuan, C. S.; Hassan, A.; Ghazali, M. I. H.; Ismail, A. F. *J. Appl. Polym. Sci.* **2007**, *104*, 3736.

14. Zankel, A.; Chernev, B.; Brandl, C.; Poelt, P.; Wilhelm, P.; Nase, M.; Langer, B.; Grellmann, W.; Baumann, H. J. *Macromol. Symp.* **2008**, *256*, 156.
15. Nase, M.; Langer, B.; Baumann, H. J.; Grellmann, W. *J. Plast. Film Sheeting* **2009**, *25*, 61.
16. Nase, M.; Androsch, R.; Langer, B.; Baumann, H. J.; Grellmann, W. *J. Appl. Polym. Sci.* **2008**, *107*, 3111.
17. Natta, G.; Corradini, P.; Bassi, I. W. *Nuovo Cim Suppl* **1960**, *15*, 52.
18. Azzuri, F.; Flores, A.; Alfonso, G. C.; Balta Calleja, F. J. *Macromolecules* **2002**, *35*, 9069.
19. Nase, M.; Langer, B.; Baumann, H. J.; Grellmann, W. *Polym. Test.* **2008**, *27*, 1017.
20. Grellmann, W.; Bierögel, C.; Reincke, K. Plastics Wiki. Available at: http://wiki.polymerservice-merseburg.de. Accessed on November 2, 2011.
21. Amancio-Filho, S. T.; dos Santos, J. F. *Polym. Eng. Sci.* **2009**, *49*, 1461.
22. Benatar, A.; Eswaran, R. V.; Nayar, S. K. *Polym. Eng. Sci.* **1989**, *29*, 1689.
23. Benatar, A.; Cheng, Z. *Polym. Eng. Sci.* **1989**, *29*, 1699.
24. Chuah, Y. K.; Chien, L. H.; Chang, B. C.; Liu, S. J. *Polym. Eng. Sci.* **2000**, *40*, 157.
25. Frankel, E. J.; Wang, K. K. *Polym. Eng. Sci.* **1980**, *20*, 396.
26. Ghosh, S.; Reddy, R. *J. Appl. Polym. Sci.* **2009**, *113*, 1082.
27. Gutnik, V. G.; Gorbach, N. V.; Dashkov, A. V. *Fibre Chem.* **2002**, *34*, 426.
28. Nonhof, C. J.; Luiten, G. A. *Polym. Eng. Sci.* **1996**, *36*, 1177.
29. Qiu, J.; Zhang, G.; Wu, Y. *Polym. Eng. Sci.* **2009**, *49*, 1755.
30. Ramarathnam, G.; North, T. H.; Woodhams, R. T. *Polym. Eng. Sci.* **1992**, *32*, 612.
31. Sancaktar, E.; Walker, E. *J. Appl. Polym. Sci.* **2004**, *94*, 1986.
32. Tateishi, N.; North, T. H.; Woodhams, R. T. *Polym. Eng. Sci.* **1992**, *32*, 600.
33. Tolunay, M. N.; Dawson, P. R.; Wang, K. K. *Polym. Eng. Sci.* **1983**, *23*, 726.
34. Truckenmüller, R.; Cheng, Y.; Ahrens, R.; Bahrs, H.; Fischer, G.; Lehmann, J. *Microsyst. Technol.* **2006**, *12*, 1027.
35. van Wijk, H.; Luiten, G. A.; van Engen, P. G. *Polym. Eng. Sci.* **1996**, *36*, 1165.
36. Wool, R. P.; Yuan, B. L.; McGarel, O. J. *Polym. Eng. Sci.* **1989**, *29*, 1340.
37. Bach, S.; Thürling, K.; Majschak, J.-P. *Packaging Technol. Sci.* **2012**, *25*, 233.
38. Shi, W.; Little, T. *Int. J. Clothing Sci. Technol.* **2000**, *12*, 331.
39. ASTM D 1876: Standard Test Method for Peel Resistance of Adhesives (T-Peel Test), **2001**.
40. Irwin, G. R. In Proceedings of International Conference Sagamore Research, **1956**, Vol.*2*, pp 289–305.
41. Stokes, D. J., Ed. Principles and Practice of Variable Pressure/Environmental Scanning Electron Microscopy (VP-ESEM); Wiley: New York, **2008**.